Phys. Status Solidi RRL **7**, No. 9, 643–646 (2013) / **DOI** 10.1002/pssr.201307224

pss +++rapid research letters+++
www.pss-rapid.com

Is graphene on copper doped?

Alexander J. Marsden[1], Maria-Carmen Asensio[2], José Avila[2], Pavel Dudin[3], Alexei Barinov[3], Paolo Moras[4], Polina M. Sheverdyaeva[4], Thomas W. White[5], Ian Maskery[1], Giovanni Costantini[5], Neil R. Wilson[1], and Gavin R. Bell[*, 1]

[1] Department of Physics, University of Warwick, Coventry, CV4 7AL, UK
[2] Synchrotron Soleil, L'Orme des Merisiers, Saint-Aubin, 48 91192 Gif-sur-Yvette Cedex, France
[3] Elettra-Sincrotrone Trieste S.C.p.A. Strada Statale 14, 34149 Basovizza, Trieste, Italy
[4] Istituto di Struttura della Materia, Consiglio Nazionale delle Ricerche, Trieste, Italy
[5] Department of Chemistry, University of Warwick, Coventry, CV4 7AL, UK

Received 24 May 2013, revised 15 July 2013, accepted 16 July 2013
Published online 22 July 2013

Keywords graphene, CVD, Cu, doping, band gap, Dirac cone, photoemission, nano-ARPES

[*] Corresponding author: e-mail gavin.bell@warwick.ac.uk, Phone: +44 (0) 24 7652 3489, Fax: +44 (0) 24 7615 0897

Angle-resolved photoemission spectroscopy (ARPES) and X-ray photoemission spectroscopy have been used to characterise epitaxially ordered graphene grown on copper foil by low-pressure chemical vapour deposition. A short vacuum anneal to 200 °C allows observation of ordered low energy electron diffraction patterns. High quality Dirac cones are measured in ARPES with the Dirac point at the Fermi level (undoped graphene). Annealing above 300 °C produces n-type doping in the graphene with up to 350 meV shift in Fermi level, and opens a band gap of around 100 meV.

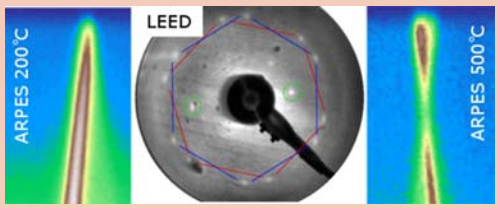

Dirac cone dispersion for graphene on Cu foil after vacuum anneals (left: 200 °C, undoped; right: 500 °C, n-doped). Centre: low energy electron diffraction from graphene on Cu foil after 200 °C anneal. Data from *Antares* (SOLEIL).

1 Introduction Graphene research continues at a frantic pace and is increasingly focused on material grown by chemical vapour deposition (CVD) on low-cost metal foils, a process readily scalable to industrial production [1, 2]. Ultra-high vacuum (UHV) surface-specific techniques such as angle resolved photoemission spectroscopy (ARPES) are ideally suited to the study of 2D materials and have been applied to graphene on single crystal surfaces [3–5]. Using spatially resolved ARPES facilities at synchrotron radiation (SR) sources [6, 7] it is possible to study single graphene grains [8, 9]. Typically, CVD-grown graphene layers comprise a patchwork of differently oriented grains: the graphene grain sizes and mismatch angles are critical for global transport and mechanical properties.

The issue of graphene doping and band-gap opening induced by substrate interaction is also crucial, both for understanding basic electronic properties and for metal contacting to graphene devices. Detailed consensus is lacking among theoretical studies of graphene-metal interactions, due to the complexity of first-principles calculations on such systems (e.g. dispersion forces, incommensurate structures) [10]. A recent ARPES study [4] found that graphene grown in UHV on Cu(111) and Cu(100) single crystals is n-doped (Fermi energy $E_F = 300$ meV above the Dirac crossing) and has an induced band-gap $E_G = 250$ meV, with both values affected by air exposure, while a recent micro-ARPES experiment found undoped graphene on Cu foil [8].

Here, we use ARPES on three different SR beamlines to clarify the doping and band gap of CVD-grown graphene on copper foil (G-Cu). We show that a gentle UHV anneal (200 °C) of air-exposed G-Cu consistently produces undoped graphene of high quality despite the presence of residual oxygen contamination. Higher temperature anneals remove some adsorbed O and begin to induce n-type doping ($E_F = 350$ meV) and the opening of a band gap ($E_G = 100$ meV).

2 Experimental Samples were grown by low pressure CVD on Cu foils. The G-Cu samples studied here comprise mm-sized copper grains with (100) surface orientation covered by a continuous patchwork of monolayer graphene grains, each grain typically several μm in size. The G-Cu structure is sufficiently ordered to produce good low energy electron diffraction (LEED) patterns: see Ref. [8] for details.

X-ray photoemission spectroscopy (XPS) and ARPES were performed on three different beamlines. Data from the beamlines are labelled *Antares*, *SM* or *VUV* for nano-, micro- and conventional ARPES respectively. In all cases samples were transferred through air without special precautions and treated in UHV only by annealing. We found that the quality of the LEED pattern correlated best with the quality of ARPES data. Experimental details and beamline information are given in the Supporting Information (online at: www.pss-rapid.com).

3 Results Spotty LEED patterns could be observed from G-Cu samples even before any thermal treatment in UHV. After gentle annealing to ~200 °C to remove physisorbed contaminants (anneal times 30 min.), a ring of spots typically became clear, as shown in Fig. 1(a). This LEED pattern is resolvable into two hexagons, each due to a set of graphene grains with consistent in-plane orientation across the whole mm-sized area probed in LEED. The two dominant graphene orientations are offset by 16° [8]. LEED spots also appear which do not move with changing beam energy: these are (00) beams from well-defined facets inclined to the Cu(100) surface plane. As the anneal temperature is increased to ~300 °C and higher, the graphene spots become weaker and more diffuse while facet spots become stronger and broader, and new facet spots may appear.

While the graphene coverage remains nearly complete (as confirmed by XPS and electron microscopy [8]), the change of LEED pattern reflects a change of the underlying structure of the facetted Cu foil. The reduction of graphene spot intensity, and increased facet spot intensity and width, are consistent with the main facet(s) becoming larger but rougher. The roughness develops on the length scale of the LEED transfer width (tens of nm) and is tracked by the graphene, lowering its diffracted intensity.

We have observed these LEED pattern changes on many G-Cu samples in different UHV systems. The ability of the Cu to restructure beneath the graphene when annealed over 200 °C is relevant to the ARPES results discussed later.

The G-Cu samples are resistant to atmospheric contamination, maintaining tarnish-free appearance for months in ambient air. Raman spectra [8] from these G-Cu samples contain *no* D-peak, indicating a very low level of defects. Their XPS spectra show only C, Cu and weak O features. Selected SR-XPS data and fitting procedures for the Cu 3p, O 1s and C 1s peaks are discussed fully in the Supporting Information and the key results summarised here.

The estimated O/C ratio is less than 10% for all samples studied, and is typically below 5%. The O/C ratio declines with increasing annealing temperature (Fig. 2). A 60 minute UHV anneal at 550 °C is sufficient to completely remove O (measured by lab-based XPS). By contrast, the Cu core levels, C 1s and C/Cu ratio hardly change during UHV annealing up to at least 500 °C, indicating that the graphene layer is stable under these conditions.

The Cu core levels can be fitted with no chemically shifted component due to CuO: fitting Cu 3p with such a component included gives an upper limit of about 1% of the total Cu peak area, though Cu_2O may also contribute. This is consistent with only a very small area of the Cu surface remaining uncovered by graphene, e.g. at Cu polycrystal surface defects [8]. The O 1s peak could be fitted with components associated with oxygen functional groups on graphene, but their binding energy range also includes CuO and Cu_2O. The C 1s XPS lines were fitted using a

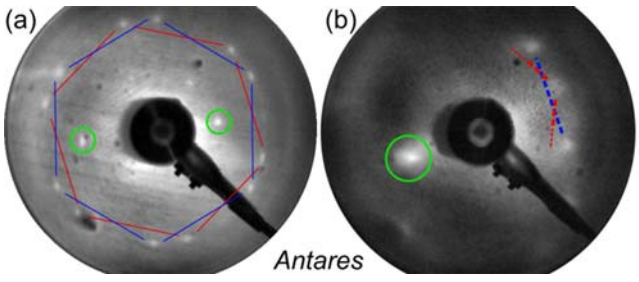

Figure 1 LEED patterns from G-Cu after anneals to (a) 200 °C [energy 70 eV] and (b) 300 °C [energy 43 eV]. In (a), the solid lines (red and blue) highlight two hexagons separated by 16° due to two orientations of graphene. The green circles highlight Cu facet spots. In (b) the graphene spots are weaker and more diffuse (dashed lines, right side) and a dominant facet appears (circled).

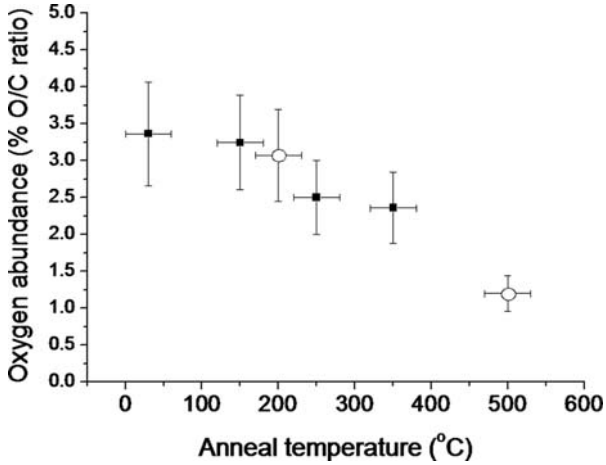

Figure 2 Oxygen abundance (O/C ratio) as a function of annealing. The abundance was estimated from SR-XPS data using only standard sensitivity factors for C 1s, O 1s and C 2p (absolute values are indicative). Shown are a single sample studied at VUV photoemission (■) and two different samples from Antares (○).

procedure based on that of Estrade-Schwarckopf, which was originally applied to oxidised graphite [11]. The C 1s peak shape is dominated by sp^2 C–C bonds, with a very small fraction (<1%) of C–O species appearing at higher binding energies and declining with increased anneal temperature.

The fitting procedures used provide consistency but are not unique. Particularly, C 1s fitting for nano-carbons is controversial and discussed further in the Supporting Information. The XPS data indicate that a nearly full coverage of graphene efficiently passivates the Cu surface against oxidation in ambient air. Similar passivation of patterned Ni films [12], Ir(111) [13] and Au–Ni(111) [14] by graphene has been reported. Oxygen contamination *during* CVD growth should be negligible due to the high temperatures under flowing H_2. Atop adsorption or intercalation of oxide species would not be distinguished by our results.

Our overall picture of the G-Cu samples is therefore as follows: the copper surface is almost completely covered by monolayer graphene with grain sizes of a few μm and oxygen is present at an O/C ratio of a few %, which declines with UHV annealing. The absence of a D-peak in Raman data [8] indicates that the graphene is not defective.

ARPES measurements were performed on G-Cu samples after different UHV annealing treatments and typical results are shown in Fig. 3. Full details and further data are given in the Supporting Information. We concentrate on the graphene K-points in the region of the Dirac cone, which terminates at the Fermi level for undoped graphene. The data show slices in reciprocal space through a Dirac cone: momentum $k = 0$ corresponds to the K-point. Panels (a) and (b) show nano-spot data ($h\nu = 100$ eV, spot size 200 nm, slice along Γ–K direction) after annealing to 200 °C and 500 °C, respectively. Figure 3(c) shows larger-area ARPES data ($h\nu = 74$ eV, sampling area 40 μm diameter, slice perpendicular to Γ–K direction).

In Fig. 3(a) and (b), individual graphene grains are probed. In (a) a very sharp band with approximately linear dispersion terminates at the Fermi level, while in (b) the band is shifted down in energy (~350 meV) and a gap has appeared (~100 meV). In Fig. 3(c), the 40 μm area probed means that tens of graphene grains should be measured simultaneously. The left panel shows raw data while the right panel shows differentiated data. Three closely spaced Dirac cones appear (one is highlighted with red lines) consistent with a collection of few-μm-sized graphene grains with a slight mutual misorientation. This is similar to rotationally shifted graphene domains observed on single crystal Ir(111) [15]. The anneal temperature was 250 °C and, as in Fig. 3(a), the Dirac cones terminate at the Fermi level, confirming the undoped nature of the graphene after only low temperature annealing. For the 40 μm probe area, the Dirac cones become weaker and less well oriented on heating ≥250 °C. Similar effects are also observed in nano- and micro-ARPES, and the sample becomes less homogeneous. This is in agreement with the evolution of the LEED pattern towards a more faceted, roughened structure.

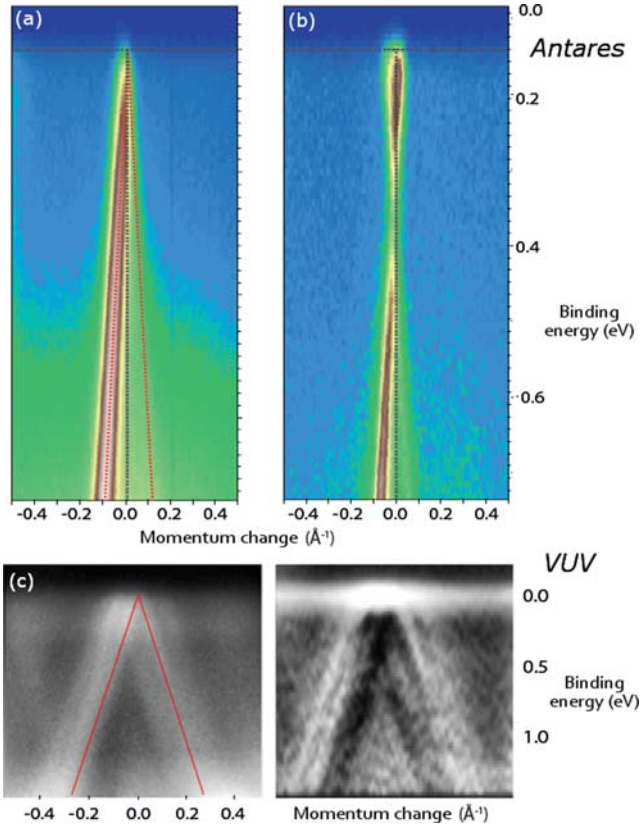

Figure 3 ARPES data near the K-point for G-Cu: (a) and (b) nano-spot data with anneal temperatures 200 °C and 500 °C, respectively; (c) 40 μm spot size, anneal temperature 250 °C (left is raw data, right panel is differentiated). In (a, b) black lines show the Fermi level and $k = 0$ while red lines are TB model fits.

The Fermi levels were found by fitting the energy distribution curves (EDCs) and the bands shown in Fig. 3 were fitted to a tight binding model [16] (nearest-neighbour only, hopping energy 3.3 eV), giving a Fermi velocity $v_F = 3.3 \times 10^6$ ms^{-1}. The induced gap seen in Fig. 3(b) was estimated from the EDCs to be 100 meV. Similar results to those shown in Fig. 3(a) and (b) were obtained performing single-grain ARPES with a 2 μm spot size and $h\nu = 74$ eV (see Supporting Information).

4 Discussion The ARPES data all indicate that the low temperature annealed G-Cu samples give undoped graphene while annealing to ≥300 °C induces a gap and n-doping. It is important to note that these results are consistent across three different UHV systems and so should not be strongly affected by, for example, adsorption of active species due to different vacuum conditions in the preparation chambers.

With $E_F = 250$ meV above the conduction band minimum for n-type graphene and $v_F = 3.3 \times 10^6$ ms^{-1}, the sheet charge density of the 500 °C annealed sample is estimated to be 4×10^{11} cm^{-2}. This is two orders of magnitude less than the density of O atoms on the graphene surface (1%

coverage $= 7.3 \times 10^{12}$ cm^{-2}). Furthermore, doping is not correlated to O abundance across our set of around 10 different G-Cu samples. Instead, the typical behaviour is as described: after a low-temperature anneal to 200–250 °C, graphene appears undoped independent of the measured O/C ratio in the range 3% to 5%. Hence, oxygen contamination may only have an indirect effect on doping and the adsorbates themselves are unlikely to dope the graphene. While we see no evidence for intercalation of oxygen between the graphene and Cu substrate, in contrast to that reported for Cu(100) in Ref. [4], the present measurements do not rule out O intercalated between the graphene and forming chemical bonds only with the graphene.

Chemical interaction between pristine graphene and single crystal substrates was shown to both alter the doping level and induce a gap by metal d-state hybridization and symmetry-breaking of the graphene sub-lattice [5, 10]. In our samples, we do not see such effects after low temperature anneals but doping and an induced band gap do arise for higher temperature annealing. This is accompanied by both a reduction in O content and an evolution of the surface towards a more faceted and inhomogeneous structure, as measured by both LEED and nano-ARPES. This symmetry-breaking may be lifted by O locally distorting the graphene structure, whether intercalated or adsorbed atop. The symmetry-broken interface and associated band gap could then form after higher temperature annealing due to O removal. This would explain both the lack of correlation between O/C ratio and initial doping: sufficient O contamination simply lifts the graphene/substrate interaction and does not directly dope the graphene. Alternatively, the local Cu facet structure may be altered by the higher temperature annealing such that a stronger Cu-graphene electronic interaction arises, leading to the doping and band gap.

Similar doping and band-gap effects are not observed on air-exposed single-crystal Ir(111) [13] or Au–Ni(111) [14]. This further suggests that the oxygen contamination indeed only plays an indirect role in the present case. Interestingly, the interaction strength and doping type for Au on graphene have recently been shown to vary depending on the *configuration* of the Au (nano-particles vs. thin films) [17]. Since Cu atoms beneath the graphene in G-Cu are sufficiently mobile to completely alter the LEED pattern after modest UHV annealing, a configurational effect could also contribute to the changes observed here. It is clear from the LEED pattern evolution that structural changes take place over a range of length scales. The large scale faceting prevents observation of local G-Cu registry by LEED alone, and further microscopic investigation of the surface evolution would be valuable. However, it is plausible that the polycrystallinity of the Cu foil substrate and the complex grain and facet structures [8] are important in allowing reconfiguration of the graphene-substrate interface on annealing. Such reconfiguration is blocked on single-crystal substrates.

5 Conclusions In summary, by comparing a large sample set measured on three different synchrotron beamlines, we have shown consistently that graphene grown by CVD on copper foil, exposed to ambient air and annealed in vacuum to 200 °C, is undoped with an ideal gapless band structure around the K-point. However, higher temperature annealing (300–500 °C) induces a significant gap and n-type doping.

Acknowledgements This work is supported by EPSRC (UK), via the Doctoral Training Grant, the Warwick Centre for Analytical Sciences (EP/F034210/1), the ULISSE project (EP/G044864/1) and an Overseas Travel Grant (EP/K005200/1). We acknowledge support via the CALIPSO TransNational Access Program and the European Science Foundation (ESF) under the EUROCORES Program Euro-GRAPHENE.

References

[1] X. Li et al., Science **324**, 1312 (2009).
[2] M. Batzill, Surf. Sci. Rep. **67**, 83 (2012).
[3] S. Y. Zhou, G.-H. Gweon, A. V. Fedorov, P. N. First, W. A. De Heer, D.-H. Lee, F. Guinea, A. H. Castro Neto, and A. Lanzara, Nature Mater. **6**, 770 (2007).
[4] A. L. Walter, S. Nie, A. Bostwick, K. S. Kim, L. Moreschini, Y. J. Change, D. Innocenti, K. Horn, K. F. McCarty, and E. Rotenberg, Phys. Rev. B **84**, 195443 (2011).
[5] A. Varykhalov, M. R. Scholz, T. K. Kim, and O. Rader, Phys. Rev. B **82**, 121101(R) (2010).
[6] A. Barinov, P. Dudin, L. Gregoratti, A. Locatelli, T. O. Mentes, M. A. Nino, and M. Kiskinova, Nucl. Instrum. Methods Phys. Res. A **601**, 195 (2009).
[7] J. Avila, I. Razado-Colambo, S. Lorcy, B. Lagarde, J.-L. Giorgetta, F. Polack, and M. C. Asensio, J. Phys.: Conf. Ser. **425**, 192023 (2013).
[8] N. R. Wilson et al., Nano Res. **6**, 99 (2013).
[9] P. Sutter, M. S. Hybertsen, J. T. Sadowski, and E. Sutter, Nano. Lett. **9**, 2654 (2009).
[10] E. Voloshina and Y. Dedkov, Phys. Chem. Chem. Phys. **14**, 13502 (2012).
[11] H. Estrade-Szwarckopf, Carbon **42**, 1713 (2004).
[12] B. Dlubak et al., ACS Nano **6**, 10930 (2012).
[13] A. Varykhalov, D. Marchenko, M. R. Scholz, E. D. L. Rienks, T. K. Kim, G. Bihlmayer, J. Sánchez-Barriga, and O. Rader, Phys. Rev. Lett. **108**, 066804 (2012).
[14] D. Marchenko, A. Varykhalov, A. Rybkin, A. M. Shikin, and O. Rader, Appl. Phys. Lett. **98**, 122111 (2011).
[15] D. Marchenko, J. Sánchez-Barriga, M. R. Scholz, O. Rader, and A. Varykhalov, Phys. Rev. B **87**, 115426 (2013).
[16] S. Reich, J. Maultzsch, C. Thomsen, and P. Ordejón, Phys. Rev. B **66**, 035412 (2002).
[17] Y. Wu et al., Small **8**, 3129 (2012).

